

Cement Hydration: Building Bridges and Dams at the Microstructure Level

by

Dale P. Bentz
Building and Fire Research Laboratory
National Institute of Standards and Technology
Gaithersburg, MD 20899 USA

**Reprinted from Knud Hojgaard Conference on Advanced Cement-Based Materials:
Research and Teaching, pp.135-146, 2005.**

**NOTE: This paper is a contribution of the National Institute of Standards and
Technology and is not subject to copyright.**

NIST

National Institute of Standards and Technology
Technology Administration, U.S. Department of Commerce

Materials: Research and Teaching
Lyngby, Denmark

Knud Højgaard Conference on Advanced Cement-Based Materials: Research and Teaching
12-15 June 2005, Technical University of Denmark, Lyngby, Denmark

Technical University of Denmark
Lyngby
45 88 32 82
sa@byg.dtu.dk
reserved.

705 København V, Denmark
Ole Mejlhede and H. Stanger

*files provided by the individual
authors or implied, with regard to the
not accept any legal responsibility*

**Knud Højgaard Conference on
Advanced Cement-Based Materials:
Research and Teaching**

Lyngby, Denmark

12-15 June 2005

**Edited by
Ole Mejlhede Jensen, Mette Geiker and Henrik Stang**
Technical University of Denmark

Cement Hydration: Building Bridges and Dams at the Microstructure Level

Dale P. Bentz

Building and Fire Research Laboratory, National Institute of Standards and Technology, USA

Abstract

The concurrent goals of cement hydration are to percolate (bridge) the original cement particles into a load-bearing network and to depercolate (dam) the original water-filled capillary porosity. The initial volume, particle size distribution, and flocculation/dispersion state of the cement particles have a large influence on both hydration rates and microstructure development. Likewise, the capillary porosity as characterized by its pore size distribution, percolation state, and saturation state also influences both hydration kinetics and microstructure. In this paper, experimental techniques and computer modeling are applied to further understanding several of the critical connections between these physical parameters and performance properties. First, the setting or bridging process is explored via a combination of needle penetration and rheological measurements, in concert with three-dimensional microstructural modeling. Second, low temperature calorimetry is shown to be a valuable indicator of the percolation state or damming of the water-filled pores with various size entryways in the three-dimensional microstructure. Porosity percolation (or depercolation) is shown to be strongly influenced by both curing conditions and the alkali content of the cement pastes. Finally, it is proposed that future efforts in this field be directed towards a greater understanding of the (nano)structures of cement hydration products, particularly the calcium silicate hydrate gel, and their influence on performance properties.

1. Introduction

As with all materials, the microstructures of cement pastes, mortars, and concretes provide the bridges between materials processing and engineering properties. Unlike many other materials, however, cement-based materials exhibit a highly dynamic (micro)structure that is extremely sensitive to initial conditions, processing, and environmental exposure. There are few materials where water plays such a critical role in processing, microstructure development, performance, and durability. In cement-based materials, water is the liquid that provides flowability to the raw materials, serves as a vehicle for and participant in the numerous and complex cement hydration reactions, exerts forces on the solid components of the porous microstructure during self-desiccation, drying, freezing, alkali-silica gel formation, and

exposure to fire, and provides the pathways for the ingress of deleterious ions. From a geometrical/structural viewpoint, the characteristics of both the porosity where the water resides and of the particles initially present in the mixing water are critical influences on hydration rates, microstructure, and performance properties. In analogy to large scale construction, cement hydration can be viewed as the process of building bridges to connect cement particles and dams to disconnect the water-filled capillary pore space.

Because many of the cement hydration products form around the initial cement clinker particles, as shown in Figure 1, the initial configuration of these particles is crucial in providing a "scaffold" on which a network of (porous) solid bridges will form. Thus, the initial water-to-cement ratio (w/c) [1], particle size distribution [2-4], and dispersion/flocculation state [5] of the particles all exert major influences not only on the developed microstructure (through and beyond setting) but also on the hydration kinetics. The bridging process can be conveniently explored via a coordinated experimental and computer modeling approach, as will be demonstrated in this paper.

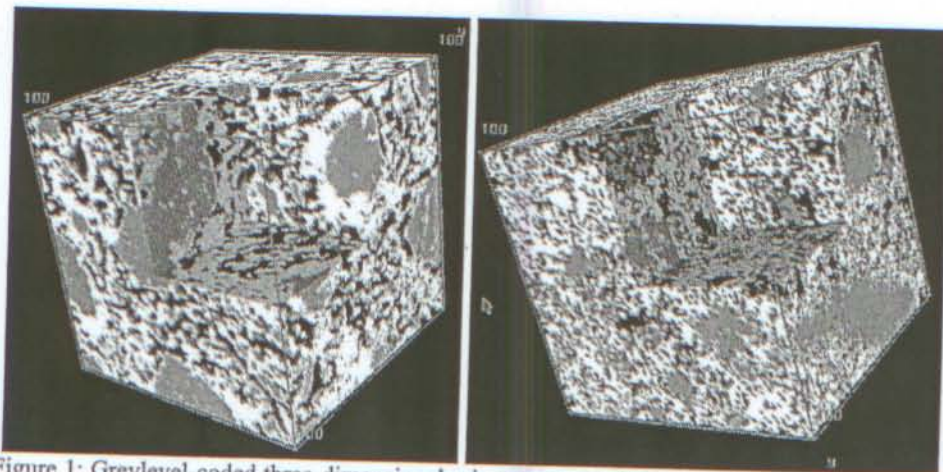


Figure 1: Greylevel-coded three-dimensional microstructures ($100 \mu\text{m} \times 100 \mu\text{m} \times 100 \mu\text{m}$) of real (left) and model (right) hydrating cement pastes of Cement and Concrete Reference Laboratory cement 133 with a $w/c \approx 0.47$ and a degree of hydration of about 0.62. Light grey represents unhydrated cement particles, white hydration products, and dark grey capillary porosity. The real microstructure was captured by x-ray microtomography at beam line ID 19 of the European Synchrotron Research Facility in Grenoble, France, in September 2000 [6, 7].

While the microstructural bridges are critical for strength development and mechanical properties, the microstructural dams are more important for limiting transport and improving the durability of cement-based materials. As cement hydration connects the original cement particles together, it may also disconnect the water-filled capillary porosity, at least at the micrometer scale. Because there are nanometer-sized pores present in the calcium silicate hydrate gel (C-S-H) hydration product, the porosity always remains percolated at the

nanometer scale [8]. Although the microstructures in Figure 1 appear disconnected, they are still highly connected. But, as for fresh pastes, sufficient hydration will result in a percolated network of C-S-H. Here, this depercolation, along with the role of the water, will be examined experimentally using

2. Experimental

Cement pastes were prepared using high proficiency cement samples 140 [1]. Detailed procedures have been provided in detail elsewhere. Cement and water were mixed in a mortar and pestle, and analyzed using a Vicat needle. Here, this depercolation, along with the role of the water, will be examined experimentally using

Cement pastes were prepared using high proficiency cement samples 140 [1]. Detailed procedures have been provided in detail elsewhere. Cement and water were mixed in a mortar and pestle, and analyzed using a Vicat needle. Here, this depercolation, along with the role of the water, will be examined experimentally using

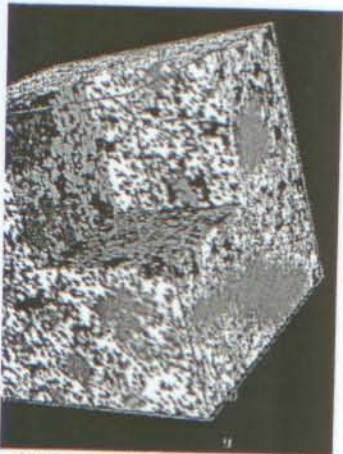
of low speed mixing while the cement contains the water, 30 s of high speed mixing water was either distilled water prepared by dissolving the relevant pore fresh paste was used for Vicat needle (about 26°C) and rheological measurements cast into small ($\approx 5 \text{ g}$) wafers that were (small amount of water on top) or sealed at 20°C . Limited repeatability tests have of the cement paste as measured by the 5 % [16-18]. At various ages, the samples were ground in a mortar and pestle, and analyzed using and/or LTC to investigate their pore structure assuming an uncertainty of 0.001 g in weight at 105°C and 1000°C , the estimated error is 0.004 [14]. For temperatures between 20°C and 100°C , the experiment has specified a constant calorimetric noise of $1.5 \mu\text{W}$.

3. Computer Modeling

All simulations were conducted using a computer model. Starting microstructures that match the composition, and phase distribution of the agents were used in the experiment, and simulated by randomly moving and aggregating particles to simulate hydration [5]. Hydration simulation was performed by monitoring the percolation of the solids was monitored [20]. During the percolation evaluation, the model was updated to be connected unless they are bridged by C-S-H or one of the aluminate hydrates.

ness of deleterious ions. From a
with the porosity where the water
g water are critical influences on
ties. In analogy to large scale
ness of building bridges to connect
illary pore space.

around the initial cement clinker
ese particles is crucial in providing
ill form. Thus, the initial water-to-
dispersion/flocculation state [5] of
veloped microstructure (through and
ding process can be conveniently
modeling approach, as will be



s (100 μm x 100 μm x 100 μm) of
Cement and Concrete Reference
dration of about 0.62. Light grey
roducts, and dark grey capillary
rotomography at beam line ID 19
France, in September 2000 [6, 7].

th development and mechanical
limiting transport and improving
tion connects the original cement
capillary porosity, at least at the
es present in the calcium silicate
ways remains percolated at the

nanometer scale [8]. Although the capillary pores present in both the real and model microstructures in Figure 1 appear depercolated in two dimensions, in three dimensions, they are still highly connected. But, as first noted by Powers many years ago [9], for lower w/c pastes, sufficient hydration will result in depercolation of the initial water-filled capillary pores. Here, this depercolation, along with the role of curing conditions and cement alkali content, will be examined experimentally using low temperature calorimetry (LTC).

2. Experimental

Cement pastes were prepared using Cement and Concrete Reference Laboratory (CCRL) proficiency cement samples 140 [10] and 152 [11]. Since many of the experimental procedures have been provided in detail elsewhere [12-14], they will only be reviewed briefly here. Cement and water were mixed in a high speed blender using the following protocol: 30 s of low speed mixing while the cement powder is introduced into the mixing vessel that already contains the water, 30 s of high speed mixing, a rest of 150 s while the sides of the mixing vessel are scraped down, and 30 s more of high speed mixing to prepare the final product. The mixing water was either distilled water or a solution of alkalis (sulfates or hydroxides), prepared by dissolving the relevant potassium and sodium compounds in distilled water. The fresh paste was used for Vicat needle penetration [15] measurements at laboratory temperature (about 26 °C) and rheological measurements by the stress growth technique [16-18] at 20 °C, or cast into small (≈ 5 g) wafers that were placed in capped plastic vials and cured under saturated (small amount of water on top) or sealed conditions in an environmental chamber maintained at 20 °C. Limited repeatability tests have indicated that the calculated values for the yield stress of the cement paste as measured by the stress growth technique have a standard uncertainty of 5 % [16-18]. At various ages, the specimens were removed from their vials, crushed using a mortar and pestle, and analyzed using loss-on-ignition (LOI) to assess the degree of hydration and/or LTC to investigate their pore structure. Based on a propagation of error analysis and assuming an uncertainty of 0.001 g in the mass measurements made initially and after heating at 105 °C and 1000 °C, the estimated uncertainty in the LOI-calculated degree of hydration was 0.004 [14]. For temperatures between -100 °C and 500 °C, the LTC equipment manufacturer has specified a constant calorimetric sensitivity of ± 2.5 % and a root-mean-square baseline noise of 1.5 μW .

3. Computer Modeling

All simulations were conducted using the CEMHYD3D V3.0 computer programs [19]. Starting microstructures that matched the measured w/c, particle size distribution, phase composition, and phase distribution of cement 152 were created. Because no water-reducing agents were used in the experiment, the digitized spherical cement particles were flocculated, by randomly moving and aggregating together the individual cement particles prior to hydration [5]. Hydration simulations were conducted under sealed conditions and the percolation of the solids was monitored to compare to the physical measurements of setting [20]. During the percolation evaluation, two touching (flocculated) particles are not considered to be connected unless they are bridged by some volume of hydration products, specifically the C-S-H or one of the aluminate hydration products [2, 5, 20]. The volume fractions of the total

solids and of the connected solids, defined as those bridging from one side of the microstructure to the opposite one, averaged over the three principal directions, was recorded as a function of hydration cycles. For hydration at 25 °C, a conversion factor of 0.00035 h/cycle² was used to convert between hydration cycles (squared) and real time [13].

4. Results and Discussion

4.1 Bridge Building: Percolation of Solids and Setting

Several previous studies have shown a quantitative relationship between setting as measured by the Vicat needle method [15] and the percolation of the solids in a three-dimensional microstructural model [20, 21]. For the standard ASTM technique [15], the Vicat measurements are generally made on a rather low (< 0.3) w/c cement paste. It is expected that the setting process would be a strong function of w/c [16-18], as the bridges being constructed to connect the particles together will generally need to be longer and/or fewer bridges per unit hydration of cement will be created when the w/c is increased.

Experimental and computer modeling results examining four different views of the "setting" process are provided in Figures 2 and 3. Figure 2 compares experimental measurements of the yield stress via stress growth measurements [16-18] with the computer modeled volume fractions of total solids, both as a function of hydration time for cement pastes with three different w/c (the stress growth measurement technique could not be applied to the w/c=0.3 cement pastes due to its high initial stiffness). As the cement particles flocculate together following mixing, they form a weak solid skeleton that is strengthened and reinforced by the cement hydration products. For a high enough w/c, this initial skeleton can not support itself under gravity so that settlement and bleeding will occur. In fact, minor bleeding was observed for the w/c=0.45 cement paste prepared with CCRL cement 152, and the initial yield stress values in Figure 2 are quite low. As the w/c is lowered to 0.4 and then to 0.35, the measured yield stress becomes higher as a greater applied stress is necessary to get the (greater number of) particles moving in the more concentrated suspensions. Initially, the model-predicted solids volume fraction and the measured yield stress track each other fairly closely, but for each w/c ratio, a point is reached where the measured yield stress climbs rapidly while the modeled volume fraction of solids continues to increase at a relatively constant and much slower rate. It is here that the percolation of the partially hydrated cement particles by the hydration products comes into play.

The bridges built by the hydration products are much stronger than the initial interparticle forces flocculating the particles together. As these bridges percolate the three-dimensional microstructure, a finite resistance to the penetration of the Vicat needle is developed, as shown in Figure 3. The time at which the needle resistance, equal to (40 mm – the needle penetration in mm), begins to increase from zero in Figure 3 is seen to correspond closely to the time when the measured yield stress begins to diverge in Figure 2. In Figure 3, the needle resistance measurements are seen to also be in general agreement with the modeled volume fraction of connected solids that characterizes the volume fraction of unhydrated cement clinker particles that are bridged by hydration products. All of this has occurred during the time when only the first 4 % to 8 % of the cement has hydrated. Already at this point, the solid skeleton is well in

place and the strength of the mic formed and existing ones are expan

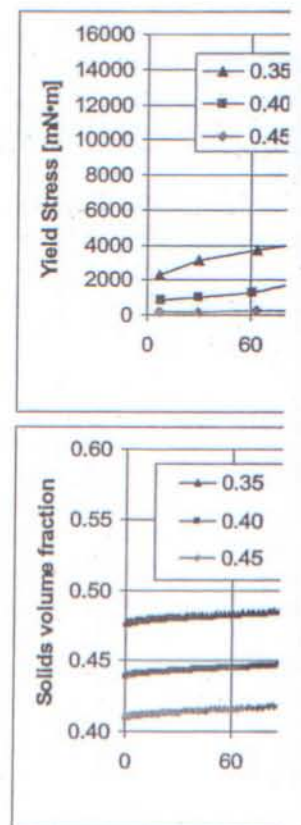


Figure 2: Two "views" of the setting process by stress growth measurements (tc

4.2 Dam Building: Depercolation Conditions and Cement Alkali C

While Powers first inferred depercolation via measurements of permeability, chemical shrinkage measurements, calorimetry scans [23-25]. A core mercury porosimetry intrusion scan is required. Generally, a percolation threshold around -15 °C [25]. Thus, the percolated or depercolated capillaries

the bridging from one side of the
 the principal directions, was recorded
 °C, a conversion factor of 0.00035
 (squared) and real time [13].

relationship between setting as measured by
 the solids in a three-dimensional
 ASTM technique [15], the Vicat
 w/c cement paste. It is expected that
 [18], as the bridges being constructed
 longer and/or fewer bridges per unit
 area.

four different views of the "setting"
 the experimental measurements of the
 with the computer modeled volume
 time for cement pastes with three
 could not be applied to the w/c=0.3
 cement particles flocculate together
 strengthened and reinforced by the
 initial skeleton can not support itself
 In fact, minor bleeding was observed
 at 152, and the initial yield stress
 0.4 and then to 0.35, the measured
 necessary to get the (greater number
 of particles. Initially, the model-predicted
 particles are packed fairly closely, but for
 the yield stress climbs rapidly while the
 volume fraction remains relatively constant and much
 lower than the initial interparticle
 volume fraction. As the solid skeleton is well in

place and the strength of the microstructure will continuously increase as new bridges are
 formed and existing ones are expanded.

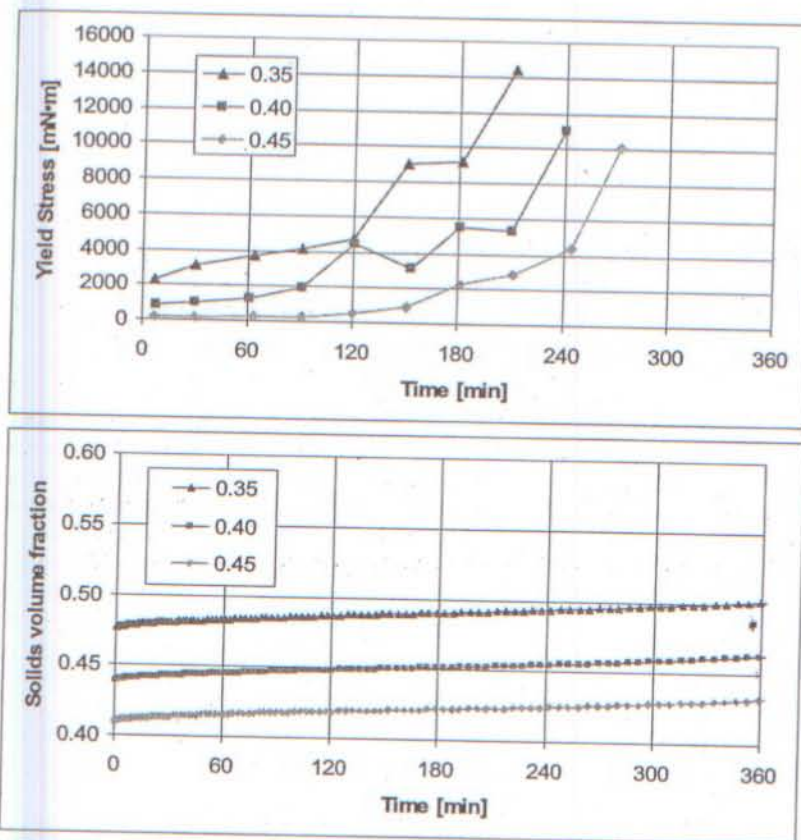


Figure 2: Two "views" of the setting process in cement paste as a function of w/c: yield stress by stress growth measurements (top) and total solids volume fraction (bottom).

4.2 Dam Building: Depercolation of Capillary Porosity and Influences of Curing Conditions and Cement Alkali Content

While Powers first inferred depercolation of the capillary porosity in hydrating cement paste via measurements of permeability [9], the depercolation can also be observed based on chemical shrinkage measurements on pastes of various thicknesses [22] or via low temperature calorimetry scans [23-25]. A cooling scan in an LTC experiment is basically equivalent to a mercury porosimetry intrusion scan [23], but with the advantage that no drying of the specimen is required. Generally, a percolated water-filled capillary pore structure is indicated by a peak around -15 °C [25]. Thus, the presence or absence of this peak can be used to infer a percolated or depercolated capillary pore structure, respectively.

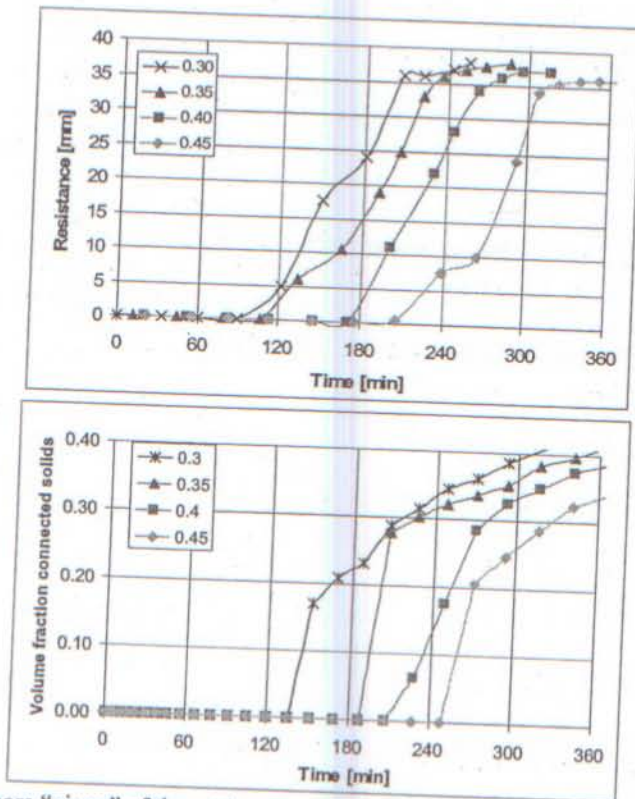


Figure 3: Two more "views" of the setting process in cement paste as a function of w/c: needle resistance (top) and connected solids volume fraction (bottom).

Figure 4 provides representative LTC scans of a w/c=0.35 cement paste cured under saturated or sealed conditions, along with scans on the pastes cured under sealed conditions after 24 h or more of resaturation. The w/c=0.35 is low enough that depercolation of the capillary pores would be expected to occur during the first week of curing [9]. For the various scans in Figure 4, basically three different peaks are observed corresponding to percolated capillary pores (freezing at about -15 °C), open gel pores (freezing at -25 °C to -30 °C), and dense gel pores (freezing at -40 °C to -45 °C) as defined in [25]. For saturated curing, the capillary pores are observed to depercolate between 3 d and 4 d of curing. Initially, a similar depercolation is observed for the capillary pores in the specimens exposed to sealed curing conditions. After a few weeks of curing, the open gel pores generally also depercolate, so that only pores accessible via the dense gel pores are detected via LTC. Specimens cured under sealed conditions are consistently seen to have smaller peaks for the capillary and open gel pores, as these larger pores are the first to empty due to chemical shrinkage and self-desiccation [12, 26].

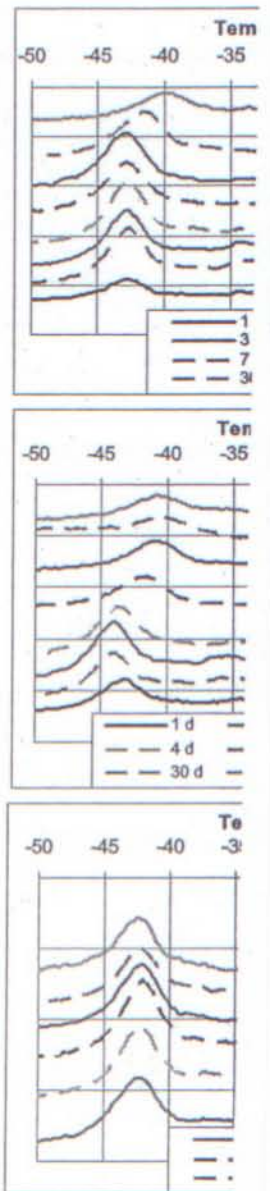
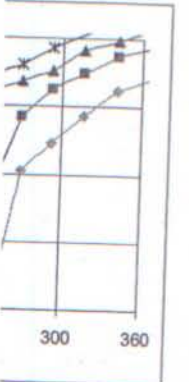
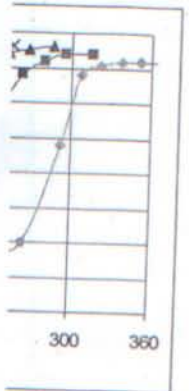


Figure 4: LTC results for CCRL cement paste cured under saturated (top) and sealed conditions for the indicated times.



paste as a function of w/c: needle
).

ment paste cured under saturated
 or sealed conditions after 24 h or
 percolation of the capillary pores
]. For the various scans in Figure
 ng to percolated capillary pores
 2 to -30 °C), and dense gel pores
 ed curing, the capillary pores are
 itially, a similar depercolation is
 sealed curing conditions. After a
 depercolate, so that only pores
 Specimens cured under sealed
 capillary and open gel pores, as
 age and self-desiccation [12, 26].

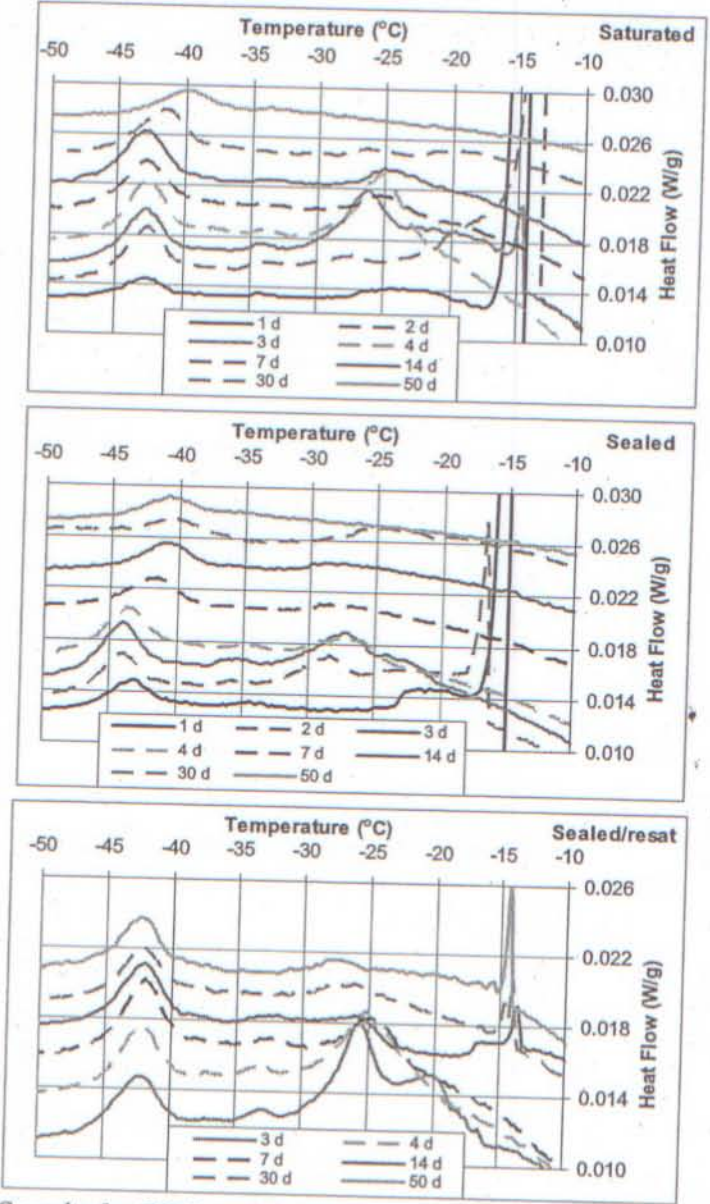


Figure 4: LTC results for CCRL cement 152 specimens (w/c=0.35, 20 °C) at various ages, cured under saturated (top) and sealed (middle) conditions and for specimens cured under sealed conditions for the indicated number of days and then resaturated (bottom) [12].

...ls a change in the percolation of the
 ...ured under saturated conditions. For
 ...epercolate, by 14 d, when resaturated,
 ...res (bottom plot for Figure 4), most
 ...the three-dimensional microstructure
 ...served by Bager and Sellevold upon
 ...ion [23]. Drying, whether external or
 ...percolated set of capillary pores (or
 ...ctron micrographs in Figure 5, the
 ...tain a set of large capillary pores
 ...nder saturated conditions. Thus, a
 ...aled/resaturated specimens is that the
 ...ways of the previously depercolated
 ...that some microcracks could also
 ...reating their own percolated network



...tron microscopy (SEM) images for
 ...ed under sealed (left) and saturated
 ...white, calcium hydroxide is light
 ...d capillary pores are black. Images

...f microstructure (specifically pore
 ...5 pastes, as illustrated by the LTC
 ...As self-desiccation occurs during
 ...ensional microstructure will empty
 ...ally not precipitate and grow in air

(or water vapor)-filled pores, hydration product formation will tend to be concentrated in the remaining smaller pores and pore entryways, where it should be more effective in depercolating the (water and vapor-filled) capillary pores [12], as supported by the experimental results in Figure 6. Thus, if curing to minimize transport and maximize durability, for an intermediate range of w/c (e.g., 0.4 to 0.45), some type of sealed/saturated curing could be superior to maintaining saturated conditions throughout. Such a seemingly counterintuitive concept is not new, having been suggested by both Swayze [27] and Powers [28] over 50 years ago.

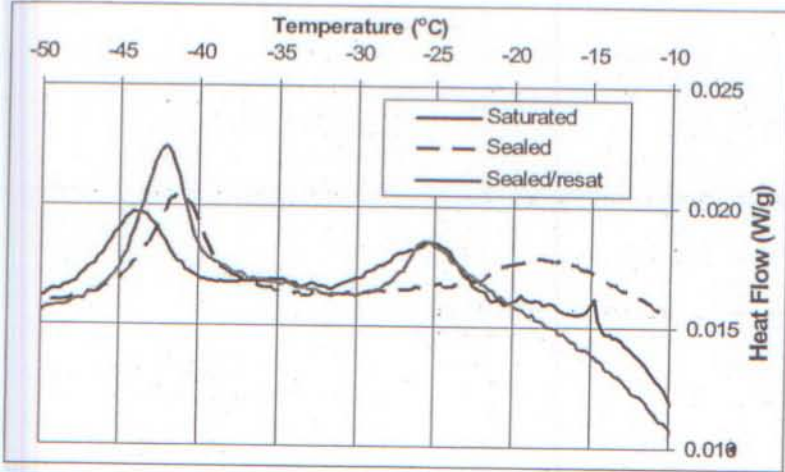


Figure 6: LTC results for CCRL proficiency cement 152 specimens (w/c=0.435, 20 °C) cured for 214 d [12].

Recently, it has been demonstrated that the percolation of the capillary porosity in hydrating cement paste can also be influenced by the level of alkalis in the cement paste [12, 14]. In the presence of sufficient alkali ions, the C-S-H has a tendency to form lath or plate-like nanostructures, with a higher degree of crystallinity [29]. Simple three-dimensional microstructure models have indicated that hydration products forming as needles or plates, as opposed to a random geometry, can be more efficient at depercolating the capillary pore space between the original cement particles [14]. In Figure 7, LTC cooling scans are provided for a set of hydrated cement pastes with and without additional alkalis, all of which have achieved nominally the same degree of hydration after 8 d of curing at 20 °C [14]. While the paste with no additional alkalis clearly contains both percolated capillary and open gel pore structures, only dense gel pores are identified in the pastes with either alkali sulfate or alkali hydroxide additions. For both additions, the same molar quantities of potassium and sodium ions (per unit mass of cement) were added to the mixing water and dissolved completely prior to the addition of the cement. This example illustrates one potential method for engineering the nanostructure of the dams formed during cement hydration.

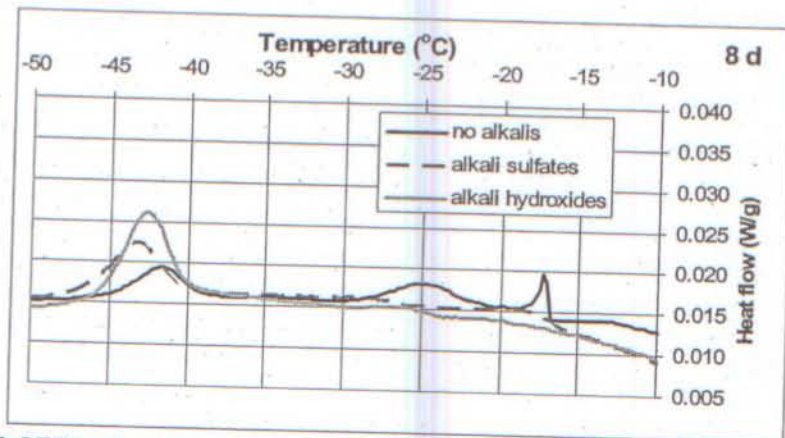


Figure 7: LTC results for CCRL cement 140 specimens ($w/c=0.40$, hydrated under saturated conditions for 8 d at $20\text{ }^{\circ}\text{C}$) with and without alkali additions (sulfates or hydroxides) [14]. All specimens have achieved basically the same degree of hydration, as measured using LOI [14].

4.3 Prospectus for Future Research — Migration from Microstructure to Nanostructure

In the future, the research focus will likely move from the microstructure created by the bridges and dams to the nanostructure of the bridges and dams themselves. For example, silica fume has a significant influence on the nanostructure of the dams, as illustrated by its large (up to 25X) influence on transport through the C-S-H gel [30]. As shown above, alkalis also definitely influence the nanostructure and crystallinity of the C-S-H gel. The nanostructure of the C-S-H gel is already being extensively studied, and atomic and nanostructure-level models are being advanced [29, 31, 32]. The ultimate engineering of the microstructure of cement-based materials will reach fruition only when the nanostructures of the bridges and dams comprising its building blocks are understood and predictable.

5. Conclusions

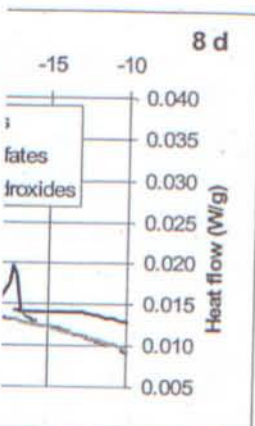
The construction of microstructural bridges and dams within hydrating cement paste has been investigated using a coordinated experimental/computer modeling approach. Bridge building is seen to be critical for the setting process, and of course also for the subsequent development of strength and mechanical properties. On the other hand, dam building is critical in depercolating the capillary porosity, leading to reduced transport coefficients and hopefully enhanced durability. Opportunities for engineering not only the nanostructure of the bridges and dams but also how they assemble at the microstructure level exist and will surely lead to innovative new materials and structures.

Acknowledgements

The author would like to thank Dr. Chiara Ferraris and Mr. John Winpigler of BFRL/NIST for obtaining and processing the needle penetration and rheological data presented in this paper.

References

1. Bentz, D.P., 'Influence of water based on spatial considerations'
2. Bentz, D.P., Garboczi, E.J., 'Ha size distribution on performance' *Concrete Research* 29 (1999) 1
3. Knudsen T., 'The dispersion concepts', *Cement and Concrete*
4. Osbaeck B., and Johansen development of portland cement (1989) 197-201.
5. Bentz, D.P., Garboczi, E.J., models to microstructure, materials', in 'The Modelling of Properties and Durability', *EC* 1996) 167-186.
6. Bentz, D.P., Mizell, S., Satterf J., Porterfield, J., Quenard, I visible cement data set', *Journ Technology* 107 (2) (2002) 137
7. Bentz, D.P., 'Quantitative correlation using correlation functions', *ac*
8. Holzer, L., Gasser, Ph., and Network in Cement Pastes Using
9. Powers, T.C., 'Capillary continuity (1959) 2-12.
10. Cement and Concrete Reference proficiency sample program: number 139 and 140', Gaithers
11. Cement and Concrete Reference proficiency sample program: number 151 and 152', Gaithers
12. Bentz, D.P., and Stutzman, I paste', submitted to *ACI Materials*
13. Bentz, D.P., 'Modeling the microstructure of CEMHYD3D', accepted by *C*
14. Bentz, D.P., 'Influence of alkali on the microstructure of cement paste', submitted to *Cement and Concrete Research*
15. ASTM C191-04b, 'Standard Test Method for Vicat Needle', *ASTM Annual Book of Standards* (American Society for Testing and Materials)
16. Amziane, S., and Ferraris, 'Influence of alkali on the microstructure of cement paste by measurements of heat flow', submitted to *ACI Materials Journal*



$w/c=0.40$, hydrated under saturated
(sulfates or hydroxides) [14]. All
ion, as measured using LOI [14].

Microstructure to Nanostructure
Microstructure created by the bridges
themselves. For example, silica fume
is, as illustrated by its large (up to
As shown above, alkalis also
C-S-H gel. The nanostructure of
micro and nanostructure-level models
of the microstructure of cement-
structures of the bridges and dams

hydrating cement paste has been
modeling approach. Bridge building
so for the subsequent development
and, dam building is critical in
transport coefficients and hopefully
by the nanostructure of the bridges
level exist and will surely lead to

John Winpigler of BFR/L/NIST for
cal data presented in this paper.

References

1. Bentz, D.P., 'Influence of water-to-cement ratio on hydration kinetics: Simple models based on spatial considerations', accepted by *Cement and Concrete Research* 2005.
2. Bentz, D.P., Garboczi, E.J., Haecker, C.J., and Jensen, O.M., 'Effects of cement particle size distribution on performance properties of cement-based materials', *Cement and Concrete Research* 29 (1999) 1663-1671.
3. Knudsen T., 'The dispersion model for hydration of portland cement 1. General concepts', *Cement and Concrete Research* 14 (1984) 622-630.
4. Osbaeck B., and Johansen V., 'Particle size distribution and rate of strength development of portland cement', *Journal of the American Ceramic Society* 72 (2) (1989) 197-201.
5. Bentz, D.P., Garboczi, E.J., and Martys, N.S., 'Application of digital-image-based models to microstructure, transport properties, and degradation of cement-based materials', in 'The Modelling of Microstructure and Its Potential for Studying Transport Properties and Durability', Eds. H.M. Jennings et al. (Kluwer Academic Publishers, 1996) 167-186.
6. Bentz, D.P., Mizell, S., Satterfield, S., Devaney, J., George, W., Ketcham, P., Graham, J., Porterfield, J., Quenard, D., Vallee, F., Sallee, H., Boller, E., and Baruchel, J., 'The visible cement data set', *Journal of Research of the National Institute of Standards and Technology* 107 (2) (2002) 137-148.
7. Bentz, D.P., 'Quantitative comparison of real and CEMHYD3D model microstructures using correlation functions', accepted by *Cement and Concrete Research* 2005.
8. Holzer, L., Gasser, Ph., and Münch, B., 'Three Dimensional Analysis of the Pore-Network in Cement Pastes Using FIB-Nanotomography,' submitted, 2005. *
9. Powers, T.C., 'Capillary continuity or discontinuity in cement paste', *PCA Bulletin* 10 (1959) 2-12.
10. Cement and Concrete Reference Laboratory, 'Cement and concrete reference laboratory proficiency sample program: Final report on portland cement proficiency samples number 139 and 140', Gaithersburg, MD, March 2001.
11. Cement and Concrete Reference Laboratory, 'Cement and concrete reference laboratory proficiency sample program: Final report on portland cement proficiency samples number 151 and 152', Gaithersburg, MD, April 2004, available at <http://www.ccril.us>.
12. Bentz, D.P., and Stutzman, P.E., 'Curing, hydration, and microstructure of cement paste', submitted to *ACI Materials Journal* 2005.
13. Bentz, D.P., 'Modeling the influence of limestone filler on cement hydration using CEMHYD3D', accepted by *Cement and Concrete Composites* 2005.
14. Bentz, D.P., 'Influence of alkalis on porosity percolation in hydrating cement pastes', submitted to *Cement and Concrete Composites* 2005.
15. ASTM C191-04b, 'Standard Test Method for Time of Setting of Hydraulic Cement by Vicat Needle,' ASTM Annual Book of Standards, Vol. 04.01 Cement; Lime; Gypsum (American Society for Testing and Materials, West Conshohocken, PA, 2004).
16. Amziane, S., and Ferraris, C.F., 'Monitoring of setting evolution of cementitious materials by measurements of rheological properties and hydraulic pressure variations', submitted to *ACI Materials Journal* 2005.

17. Amziane, S., and Ferraris, C.F., 'SCC evolution of formwork hydraulic pressure and rheological properties', ACI Proceedings (New York), 2005.
18. Amziane, S., and Ferraris, C.F., 'Caractérisation de la prise des matériaux cimentaires', Proc. of the GFR convention, Mulhouse (France) October 2004 (in French).
19. Bentz D.P., 'CEMHYD3D: A three-dimensional cement hydration and microstructure development modelling package. Version 3.0', NISTIR 7232, U.S. Department of Commerce, June 2005.
20. Haecker, C.J., Bentz, D.P., Feng, X.P., and Stutzman, P.E., 'Prediction of cement physical properties by virtual testing', *Cement International* 1 (3) (2003) 86-92.
21. Princigallo, A., Lura, P., van Breugel, K., and Levita, G., 'Early development of properties in a cement paste: A numerical and experimental study', *Cement and Concrete Research* 33 (2003) 1013-1020.
22. Geiker, M., 'Studies of portland cement hydration: Measurement of chemical shrinkage and a systematic evaluation of hydration curves by means of the dispersion model', Ph.D. Thesis, Technical University of Denmark, Lyngby, Denmark, 1983.
23. Bager, D.H., and Sellevold, E.J., 'Ice formation in hardened cement paste, Part II- Drying and resaturation on room temperature cured pastes', *Cement and Concrete Research* 16 (1986) 835-844.
24. Villadsen, J., 'Hærdetemperaturens indflydelse på hærdnet cementpastas porestruktur: Projekt rapport', The Technical University of Denmark, Lyngby, Denmark, 1989.
25. Snyder, K.A., and Bentz, D.P., 'Suspended hydration and loss of freezable water in cement pastes exposed to 90% relative humidity', *Cement and Concrete Research* 34 (11) (2004) 2045-2056.
26. Bentz, D.P., Jensen, O.M., Hansen, K.K., Oleson, J.F., Stang, H., and Haecker, C.J., 'Influence of cement particle size distribution on early age autogenous strains and stresses in cement-based materials', *Journal of the American Ceramic Society* 84 (1) (2001) 129-135.
27. Swayze, M.A., 'Early concrete volume changes and their control', *Journal of the American Concrete Institute* 13 (5) (1942) 425-440.
28. Powers, T.C., 'A discussion of cement hydration in relation to the curing of concrete', *Proceedings of the Highway Research Board* 27 (1947) 178-188.
29. Richardson I.G., 'Tobermorite/jennite- and tobermorite/calcium hydroxide-based models for the structure of C-S-H: Applicability to hardened pastes of tricalcium silicate, β -dicalcium silicate, portland cement, and blends of portland cement with blast-furnace slag, metakaolin, or silica fume', *Cement and Concrete Research* 34 (2004) 1733-1777.
30. Bentz, D.P., Jensen, O.M., Coats, A.M., and Glasser, F.P., 'Influence of silica fume on diffusivity in cement-based materials. I. Experimental and computer modeling studies on cement pastes', *Cement and Concrete Research* 30 (2000) 953-962.
31. Nonat, A., 'The structure and stoichiometry of C-S-H', *Cement and Concrete Research* 34 (2004) 1521-1528.
32. Cong, X., and Kirkpatrick, R.J., ' ^{29}Si MAS NMR study of the structure of calcium silicate hydrate', *Advanced Cement-Based Materials* 3 (1996) 144-156.

Strength Development and at Early Age

Kiyofumi Kurumisawa and Toyohar
Graduate school of engineering, Hol

Abstract

Strength development of fly ash-c
Strength development of cementit
However, there have been few
development and microstructure of
condition on compressive and bend
microstructures at early ages, were
electron image method. From the r
development and microstructure w:
ash.

1. Introduction

Fly ash is increasing in Japan as
disposal of fly ash becomes a p
Therefore, it was thought that it v
material. However, while fly ash
development and fluidity etc. when
is the disadvantage of the delay
development of concrete with fly
Therefore, the curing temperature i
additives for activating the reactio
microstructure on initial strength d
development of cement-based mat
point of view.